Testing for Photocorrosion of Earth-Abundant Metal Oxides with Optical Band-Pass Filters

Angelina Ye*[1], Caitlyn S. Delgadillo[2]

[1]Northwood High School with Concordia SEAL, Concordia University, Concordia, Irvine, California 92612, United States

[2] Alverno High School, N Michillinda Ave, Sierra Madre, California 91024, United States

ABSTRACT: In the context of solar fuels, a metal oxide photocatalyst is needed to catalyze water splitting to convert solar energy to chemical energy in a cost-effective, efficient manner. The SEAL (Solar Energy Activity Lab) kit tests for photoactivity of researcher-chosen, earth-abundant photocatalysts by illuminating them on a plate with a layer of conductive fluorine-doped tin oxide (FTO) and measuring the resulting current. However, it must be determined if the current detected by the kit is due to the photoactivity of the metal oxide instead of its photocorrosion. To do this, band-pass, color substrate filters of different colors were placed over the white light LED array to limit the transmitted light to a certain range of wavelengths. The filters tested if photoactivity was detected beginning with the specific wavelength correlating to the metal oxide's band gap, or if it occurred at longer wavelengths, signifying photocorrosion. Iron nitrate, cobalt nitrate, nickel nitrate, and copper nitrate were spotted in patterns on FTO plates and then annealed to form iron oxide, cobalt oxide, nickel oxide, and copper oxide, which were tested with the SEAL kit. The data confirmed current onset occurred at wavelengths correlating to the metal oxide band gap, implying that photoactivity, not photocorrosion, most likely contributes to the majority of the SEAL kit current.

1. INTRODUCTION

Solar energy has the most abundantly available renewable energy since the sun beams energy to the vast majority of the earth[1-6]. The energy from 40 minutes of the sunlight that reaches Earth is equivalent to the world's current annual energy consumption[2,3]. However, solar energy is currently utilized as strictly diurnal photovoltaic panels that are inhibited by clouds or darkness and lose energy from converting to direct current electricity[1,2,4]. As such, the panels only operate at maximum capacity 20% of the time[1,2]. To create constant solar fuel generators, photocatalytic semiconductors are needed to catalyze water splitting, which turns the solar energy into chemical energy in the form of hydrogen and oxygen gas[4-7]. To create usable energy, either the hydrogen gas can be used as a fuel by itself or the hydrogen and oxygen can combine to form water in a fuel cell, releasing energy as an exothermic reaction[2,5,6]. The semiconductors tested in the Solar Energy Activity Laboratory (SEAL) kit are limited to earth-abundant metals in the form of metal oxides to optimize production, performance, and cost-effectiveness[4,6].

The SEAL kit tests for 2 ideal components of a fuel-forming photoelectrocatalyst: the light absorbance and the catalytic properties[4,7]. An 8 by 8 square array of pulsing LEDs illuminates metal oxide spots on a transparent, conductive, fluorine-doped tin oxide (FTO) plate (Figure 1)[4,6]. The current integrator unit measures the photoactivity, which is then analyzed by the custom "Soar Material Discovery" (SMD) program made by Dr. Jay Winkler and Gates Winkler[8]. The program displays the detected photocurrent of each individual spot[8]. Substances such as bismuth vanadate and a mixture of iron oxide with nickel oxide have performed well with the kit, while iron oxide is used as a standard control[6,9,10].

Since the SEAL kit only detects photocurrent, it was uncertain if the current is due to the photoactivity of the spot or photocorrosion. If the current was from photocorrosion, it could have potentially signified the inaccuracies of the results from the SEAL kit scans and might have required an alternative testing method than SEAL. Knowing the band gaps of the tested metal oxides can help evaluate the accuracies of the SEAL kit, and possibly distinguish the current from photoactivity and that of photocorrosion. The inverse relationship between the energy of a photon (eV) and its wavelength (μm) was used to determine the threshold wavelength required to pass the band gap. To control what wavelengths are transmitted, a band-pass filter was placed over the LED array emitting white light. By transmitting a specific range of wavelengths, the metal oxide was analyzed for photoactivity at predicted wavelength according to the band gap. The effects of transmitting shorter, more energetic wavelengths and using metal oxides with lower band gaps on the photocurrent were also analyzed. The use of filters also helped identify the relationship between mixed metal oxides, and their photoactivity and band gap.

2. EXPERIMENTAL SECTION

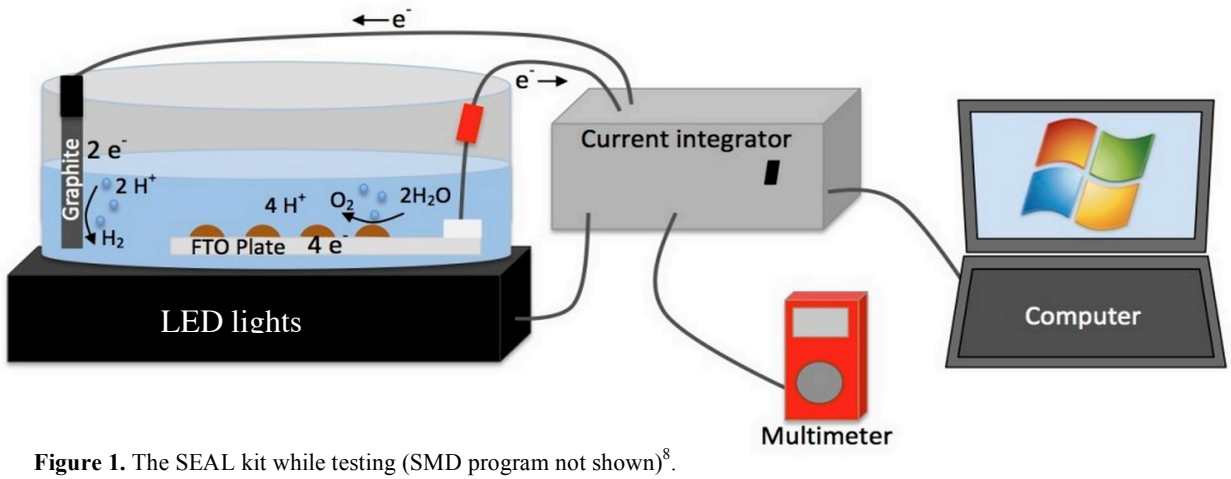

Figure 1. The SEAL kit while testing (SMD program not shown)[8].

2.1. SEAL Kit. The SEAL kit was used to test the photoactivity of metal oxides (Figure 1). In order to prepare the metal oxide samples, metal nitrates were spotted onto glass plates with conductive fluorine-doped tin oxide (FTO) on one side. The plates are then air dried and placed into a kiln to anneal, leaving a metal oxide. Then, a copper wire was attached to the FTO plate by copper tape and covered by epoxy to prevent extraneous current. The SEAL kit was operated by connecting the integrator box with the voltmeter and a set of 64 pulsing LED lights in an 8 by 8 pattern. The plate with the dried epoxy was placed in a crystallization dish with a graphite rod taped to the side. A solution of 0.1 M NaOH was poured to cover the plate and the bottom of the graphite rod. The integrator box was then turned on, then the voltmeter was turned on and set to 2 DCV. Subsequently, the SMD (Solar Materials Discovery) program was turned on. To calibrate the voltmeter to the program, the initial reading of the voltmeter was inputted. The working electrode of the integrator box was connected to the copper wire on the plate and the counter electrode was attached to the graphite rod. A voltage of 0.100 V was then applied, and after the dark current was below 0.5 V, a 3-cycle scan was run with the program. The LED lights flashed and illuminated the spots, prompting them to catalyze using the light energy and create photoactivity through current. The data collected by the SMD program was saved after inputting the experiment information.

2.2. Annealing. After spotting, all plates were air-dried to until fully or at least partially dry. They were placed inside an Evenheat Set-Pro kiln to anneal. The kiln was set to ramp up 363 degrees Fahrenheit every hour until it reached 932 degrees Fahrenheit (approximately 500 degrees Celsius) for 5 to 5.5 hours. The annealing process was done in atmosphere at atmospheric pressure. The annealing not only adhered the sample to the plate, but also promoted metal oxide formation.

2.3. Optical Band-pass Filters. Optical band-pass filters were used to limit the wavelengths transmitted through the plate. Two different types of filters were used: colored glass (G) and plastic colored gelatin (P). The different glass filters were orange, green, and blue. The different plastic filters were red, orange, yellow, green, and blue. To utilize them, a filter was placed directly over the white LED lights, covering all 64 lights. The crystallization dish with the plate in a 0.1 NaOH solution was then placed directly on top of the filter and the test proceeded as described above. All 8 filters were tested with a Cary 50 UV-Vis spectrophotometer for their transmittance and absorption. The filters were placed individually inside the spectrometer and tested with the light inside the device.

2.4. Iron Controls. First, a 20 mL iron nitrate ($Fe(NO_3)_3$) solution was created by diluting iron nitrate nonahydrate crystals to 0.1 M with deionized water in a volumetric flask. Then, 20 µL of the solution was spotted onto a 3 in. by 3 in. FTO plate labeled as "CON 1" with a glass etcher (CON being an abbreviation for "control"). This occurred in a checkerboard pattern that excluded edges and the top right 3 by 2 spot corner to create a place for the copper wire and epoxy later (Figure 2a). The plate was then air dried and annealed. A copper wire of approximately 6 inches was then obtained and 0.5'' was stripped off each end. One end was placed in the empty right corner and a small piece of copper tape was placed over it to adhere it the plate. A clear 5-minute epoxy was then used to cover both the tape and wire. Once dried, the plate was scanned using the SEAL kit and no filters. Then the plate was scanned using all the glass filters in the order: orange, green, then blue. This entire scanning process was repeated for reproducibility. The results from CON 1 proved the SEAL kit functioned properly from the program showing photoactivity only where the spots were located. However, the overall average photoactivity of the spots was too low to discern enough of a difference between each of the filters.

Due to lower results, a 20 mL 0.4 M iron nitrate solution was made, and 10 µm was spotted in the same pattern on a plate labeled "CON 2". After drying and being placed in the kiln, copper wire and epoxy were applied to the top right corner. This plate was also scanned without a filter and with each glass filter twice. Then it was scanned with all the plastic filters in the order of red, orange, yellow, green, and blue.

A CON 3 plate was made later with the 0.4 M iron nitrate solution and the pattern in Figure 2a to create a new control plate in case the NaOH solution affected the other CON plates in any way. However, the spots crystallized when drying and after being heated in the kiln, formed shiny, flaky spots that

flaked off into the 0.1 M NaOH solution and left only thin rings of red iron (II, III) oxide. This plate was scanned once without a filter then with the orange glass filter, yellow plastic filter, green glass filter, and blue glass filter. As a result of the lack of material on the plate, the photo activity detected was very weak in comparison to both CON 1 and CON 2.

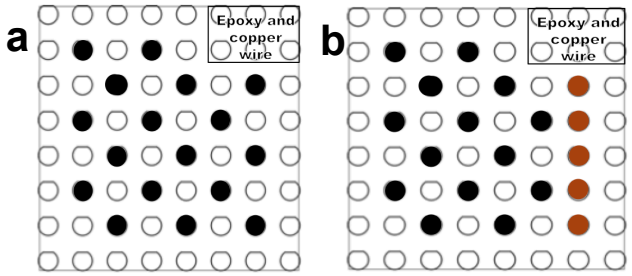

Figure 2. (a) The pattern used to spot the iron oxide control plates. (b) The pattern used to spot the other metal oxides (black) with the iron oxide control (red).

2.5. Other Metal Oxides.

2.5.1. Nickel Oxide. A 20 mL 0.4 M nickel nitrate was made and spotted onto a plate labeled "Ni 1" with 10 µm spots and a column of iron nitrate as a control (Figure 2b). However, the nickel nitrate spots did not dry in a period of 7 days and was placed on a hot plate at 55 C for an hour, then placed into the kiln. After being prepared for scanning by putting on the copper wire and epoxy, the nickel oxide was scanned only without a filter once due to its very low photocurrent due to its high band gap. Its high band gap (3.6 eV) suggested that it was not a good light absorber for the SEAL kit and would only catalyze water splitting with ultraviolet light.

2.5.2. Copper Oxide. Due to the significantly lower band gap of copper oxide (1.2 eV compared to iron oxide's 2.18 eV), a 20 mL 0.4 M copper nitrate solution was created and spotted on a plate etched "Cu 1" in the exact same fashion as the nickel. The copper nitrate, like the nickel, did not dry after several days and was placed in a desiccator for an hour, then heated in the kiln. Once cooled, it was prepared for scanning and scanned without a filter then scanned with each filter once in the order of (plastic: red, orange, yellow, green, blue, then glass: orange, green, blue). The green glass filter was used twice because the first scan showed irregular results from high photoactivity in an area where there were no spots.

2.5.3. Cobalt Oxide. Cobalt oxide was also utilized by creating a 20 mL 0.4 M cobalt nitrate solution and spotting it similarly to the other metal nitrates on a plate labeled "Co 1". This plate was also placed into a desiccator to dry and then placed in the kiln. The plate was prepared for scanning exactly the same as all the other plates. It was scanned without a filter and then scanned with each of the plastic filters in decreasing wavelength order.

2.6. Mixed Metal Oxides. A 20 mL mixture of 15.6 mL of 0.4 M $Fe(NO_3)_3$ and 4.4 mL of 0.4 M $Ni(NO_3)_3$ was made using crystallized iron nitrate nonahydrate, crystallized nickel nitrate hexahydrate, and deionized water. It was then spotted with 10 µL spots on a plate labeled as "FeNi 1" in the pattern seen in Figure 3a. After air-drying for a day, it was placed into the kiln and then prepared for scanning. It was scanned without a filter and then with all the filters. However, since none of the scans resulted in an average current of above 0.05 amps, the difference between the results from each of the filter was not very significant.

A mixture of metal nitrates was also created using 1 mL of 0.4 M $Ni(NO_3)_2$, 2 mL of 0.4 M $Fe(NO_3)_3$, and 2 mL of 0.4 M $Co(NO_3)_2$ by using a 1000 µL micropipette and pipetting from the previously made solutions into a new 20 mL vial. Using 10 µL of each solution, this mixture, 0.4 M iron nitrate, 0.4 M cobalt nitrate, and 0.4 M nickel nitrate were spotted on a plate named "HARP" in the pattern in Figure 3b. After putting epoxy on the plate, it was scanned without a filter then with only the plastic filters in order of longest to shortest wavelength.

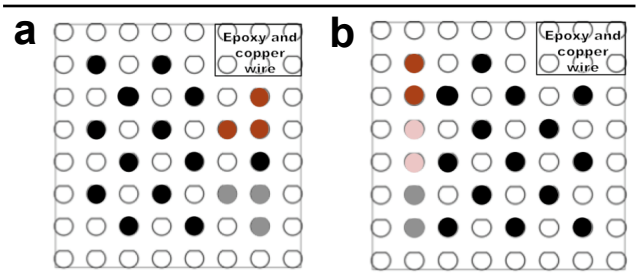

Figure 3. (a) The pattern used to spot FeNi 1; spots of the iron-nickel oxide mixture (black), iron oxide (red), and nickel oxide). (b) The pattern used to spot HARP; spots of the 1 nickel oxide: 2 iron oxide: 2 cobalt oxide mixture (black), iron oxide (red), cobalt oxide (pink), and nickel oxide (grey).

2.7. Layering Metal Oxides. Layers of metal oxides were also used. First, 10 µL of 0.4 M nickel nitrate with a column of iron nitrate as a control (Figure 2b) were spotted onto a plate labeled "NiFe 1" and placed on the hot plate to dry. After drying, the plate was heated in the kiln. Once cooled, 10 µL of iron nitrate was spotted over the nickel oxide spots. However, the spots spread to almost all the plate. After air-drying for 2 days, it was placed into the kiln to allow the iron oxide to form a red film over the majority of the plate (Figure 4a). After the copper wire and epoxy were applied, it was tested without a filter twice due to the unusually high readings and then was tested with each of the filters, first plastic and then glass in decreasing wavelength order. Finally, it was scanned without a filter once more.

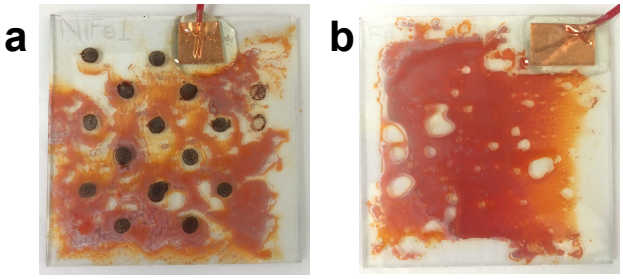

Figure 4. (a) Iron oxide layered over nickel oxide on NiFe 1 after annealing (with copper tape, copper wire, and epoxy). (b) Iron oxide spread all over plate Fe (S) after being annealed (with copper tape, copper wire, and epoxy).

2.8. Spreading Iron Oxide.

2.8.1. Single-Layer, 0.4 Molarity Iron Nitrate. To replicate the spreading effect seen in NiFe 1, a plate was ozone cleaned using the UV Ozone Procleaner Plus (Bioforce Nanoscience). It was then labelled as "Fe (S)". Using a 200 µm micropipette, 150 µL was slowly spotted onto the plate using intervals of 20 and 10 µL. The solution was spread out all over except for the edges and the top 3 by 2 rectangle for the epoxy. It was air-dried for 2 days and then put in the kiln to be annealed (Figure 4b). After applying epoxy and copper wire, the plate was scanned without a filter and then with all the glass filters in decreasing wavelength order. The scanning process was repeated without a filter and with all the plastic filters in decreasing wavelength order.

2.8.1. Double-Layer, 0.2 Molarity Iron Nitrate. In order to test the effect of layers on the photocurrent, a plate labelled "Fe (SL)" was ozone cleaned using the UV Ozone Procleaner Plus (Bioforce Nanoscience). Using a 20 µL micropipette, 80 µL of a 0.2 M iron nitrate solution was spotted onto the plate and spread over the entirety of the plate with the exception of the 3 spots by 2 spots rectangle for the copper wire and epoxy. The plate was air-dried for 2 days and then annealed in the kiln. After letting the kiln cool, the plate was taken out and immediately spotted with 80 µL of 0.2 M iron nitrate. This layer was also spread and left to air dry. After air-drying and annealing, copper wire and epoxy were applied to the plate. A foil cover was made with aluminum foil lined with paper napkins. The plate was tested twice with the foil cover (paper napkin facing the plate), twice without a cover, and twice with the cover (foil side facing the plate). Then, it was tested covered (paper napkin facing the plate) with the glass filters in decreasing wavelength order, the plastic filters in decreasing wavelength order, and then without a filter. The process was repeated once.

2.9. Testing Bismuth Vanadate. A plate was spotted with bismuth vanadate in a checkerboard pattern by another group. The bismuth vanadate solution used was made from sodium metavanadate and had a molarity of 0.05. After air-drying and annealing, the spots were white with a slight yellow tinge. The plate was tested without a filter twice.

Another bismuth vanadate plate previously made by another group was tested in the SEAL kit. However, the bismuth vanadate solution used was made from ammonium metavanadate and had a molarity of 0.1. The spots were a bright yellow (Figure 5). The plate was tested without a filter twice, then it was scanned with all the glass filters in decreasing wavelength order, with no filter, and finally with all the plastic filters in decreasing wavelength order. The scanning process was repeated once more.

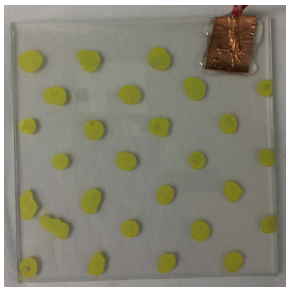

Figure 5. The 0.1 M bismuth vanadate spots made with ammonium metavandaate

3. RESULTS

3.1. Results from the Iron Oxide Control Plates. Out of all the control (CON) plates, the CON 2 produced the highest photocurrent while CON 1 and CON 3 produced lower similar photocurrents (Figure 6a,b). Iron oxide consistently resulted in the one of the highest photocurrent out of all tested metal oxides. With the filters, the control plates had low photocurrent with the longer wavelength filters. As filters that transmitted shorter wavelengths were used, the photocurrent detected in the scans also slowly rose, with the exception of the green plastic and green glass filters.

a

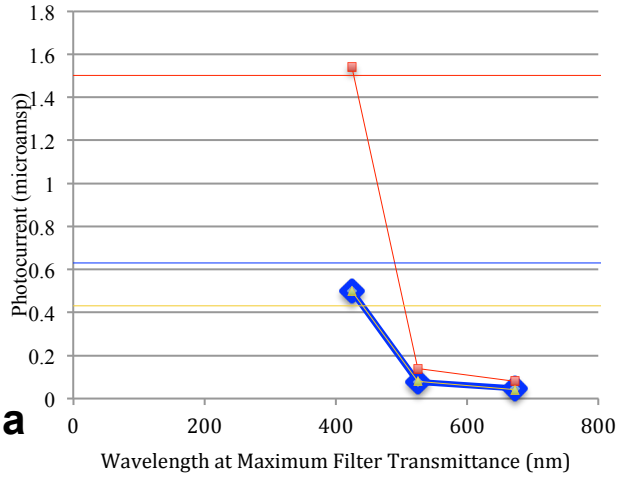

b

Filter	Maximum Transmittance	Wavelength (nm)
No filter	100%	All
Blue plastic	67.08%	411.95
Blue glass	77.38%	423.96
Green glass	27.31%	525.02
Orange glass	88.79%	672.96
Orange plastic	86.31%	684.98
Yellow plastic	87.24%	698.96
Green plastic	64.04%	699.97
Red plastic	68.30%	699.97

Figure 6. (a) Photocurrents detected from the scans with no filter (horizontal line), orange glass, green glass, and blue glass of CON 1 (blue), CON 2 (red), and CON 3 (yellow). (b) All of the filters with their maximum transmittance at the corresponding wavelength within the visible light spectrum.

Filter	Ni 1 (μA)	FeNi 1 (μA)	Cu 1 (μA)	HARP (μA)	Co 1 (μA)	CuFe: Iron Oxide (μA)	CuFe: 8:2 (μA)	CuFe: 6:4 (μA)	CuFe: 4:6 (μA)	CuFe: 2:8 (μA)	CuFe: Copper Oxide (μA)
No filter	0.05	0.18	0.24	0.04	0.05	2.09	1.39	1.40	0.87	0.96	0.36
Blue plastic		0.11	0.72	0.04	0.04	1.48	0.80	0.84	0.49	0.59	0.16
Blue glass	0.05	0.11	0.11	N/A	N/A	1.52	0.88	0.88	0.53	0.59	0.18
Green glass		0.02	0.04	N/A	N/A	0.19	0.14	0.15	0.10	0.10	0.03
Orange glass	0.03	0.03	0.1	N/A	N/A	0.38	0.37	0.37	0.31	0.23	0.09
Orange plastic	N/A	0.02	0.03	0.03	0.04	0.30	0.22	0,30	0.15	0.08	0.03
Yellow plastic	N/A	0.04	0.12	0.02	0.10	0.79	0.66	0.65	0.48	0.41	0.14
Green plastic	N/A	0.02	0.01	0.03	0.04	0.15	0.11	0.12	0.08	0.07	0.03
Red plastic	N/A	0.11	0.02	0.03	0.05	0.14	0.13	0.14	0.10	0.07	0.04

Table 1. The photocurrents of the other metal oxides and mixed metal oxides. The ratios for plate CuFe are iron oxide to copper oxide.

3.2. Results from the Other Metal Oxides and Mixed Metal Oxides. All of the other metal oxides and mixed metal oxides used (Ni 1, Co 1, Cu 1, HARP, FeNi 1, etc.) never exceeded 0.25 μA, with the exception of the CuFe plate (Table 1). The photocurrent detected from the scans with different filters were very similar and almost indistinguishable.

3.3. Results from the Layered Nickel Oxide and Iron Oxide Plate. The NiFe 1 plate produced one of the unfiltered highest photocurrents compared to the rest of the plates. Without a filter, the photocurrent detected averaged to 3.34 μA. The spots with nickel oxide had lower photocurrents, about 0.5 μA lower on average.

3.3. Results from the Bismuth Vanadate Plates. The bismuth vanadate plate made with sodium vanadate consistently produced photocurrent below 1 microamp. The bismuth vanadate plate made with ammonium metavanadate had a much higher photocurrent without a filter than the other bismuth vanadate plate tested. The scans with all the filters except for both blue filters detected photocurrent less than 0.5 μA. However, with the blue filters, the photocurrents produced by the plate were over 10 times higher than the scans with the other filters (Figure 7b). There was one outlier spot that was 50 times less than the average spot without a filter, which was omitted from the table and graph. The $BiVO_4$ plate produced the highest photocurrent without a filter out of all plates tested.

3.4. Results from the Spread Iron Oxide Plates. The photocurrent with no filter detected from the Fe (S) plate was much higher than the other iron oxide plates. However, the photocurrent from the NiFe 1 plate was higher. The scans with the blue glass filter had the highest photocurrent relative to the other filtered scans.

The photocurrent of the Fe (SL) was the second highest unfiltered photocurrent detected through this experiment (Table 7b). The scans with the blue glass filter produced the highest photocurrent compared to the other filtered scans.

3.5. Results from Covering the Plate During Testing. With Fe (SL), covering the plate with the napkin side facing the plate led to the highest photocurrent (Table 2) and consistently low dark current at approximately 0 V. The scans with the cover with the foil facing the plate produced the second highest photocurrent. However, the SEAL kit detected more photocurrent on the bottom edge than the top edge, unlike the scans with the other cover and no cover. Although the dark current was also approximately 0 V before each scan, the dark current was extremely high after each test and would only go down if the cover was lifted temporarily. The uncovered scans had the lowest photocurrent, but the distribution of photoactivity was even, similar to the napkin-lined cover.

Plate Cover	Photocurrent (μA)
No cover	3.37
Napkin-lined cover	3.82
Foil-lined cover	3.45

Table 2. The photocurrents detected from unfiltered scans of Fe (SL) without a cover and with different covers.

3.6. Results from the UV-Vis Spectrophotometer. By using the UV-Vis spectrophotometer, it was found that each of the filters had varying amounts of maximum transmittance. It was also discovered that the range of wavelengths transmitted did not all have the same transmittance and all the filters did not have clean cut-off wavelengths where they stopped transmitting (Figure 8).

3.7. Results from the Filters. As predicted, the scans with the glass blue filter produced the highest photocurrent relative to all other filters, and the scans without any filter produced the highest photocurrent overall. The order of performance of each plate from least to greatest often was from red plastic filter to blue glass filter to no filter (Figure 7a,b). However, the

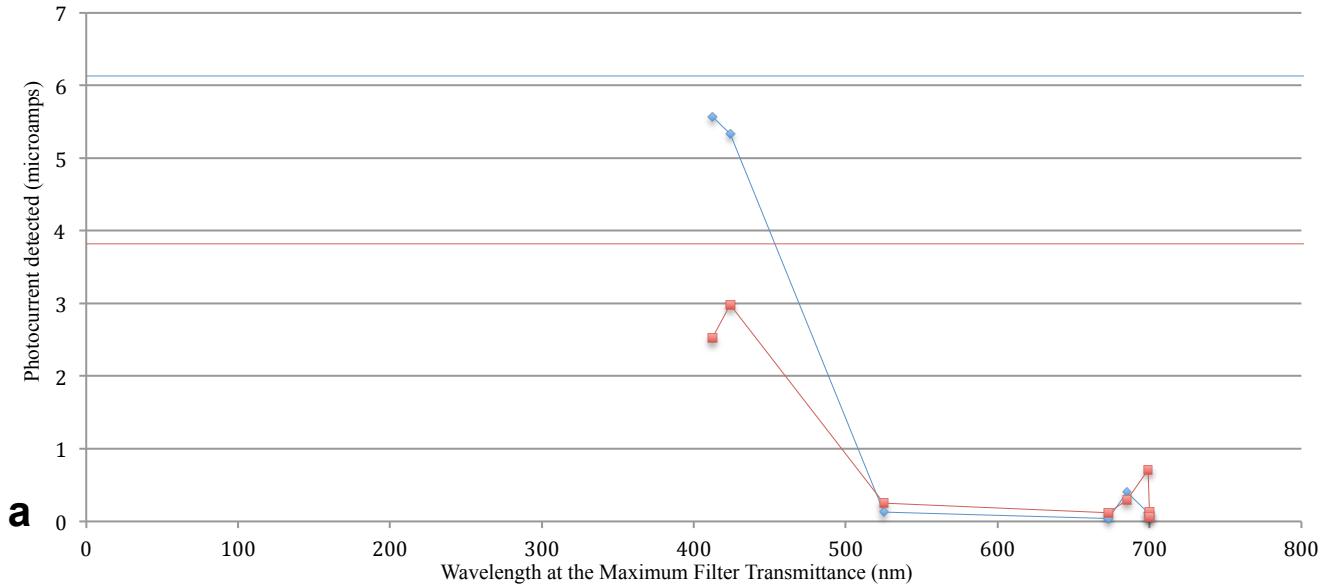

b

Filter	Maximum Transmittance	Wavelength (nm)	$BiVO_4$ (μA)	Fe (SL) (μA)
No filter	100%	All	6.13	3.82
Blue plastic	67.08%	411.95	5.57	2.52
Blue glass	77.38%	423.96	5.33	2.98
Green glass	27.31%	525.02	0.13	0.25
Orange glass	88.79%	672.96	0.04	0.12
Orange plastic	86.31%	684.98	0.40	0.30
Yellow plastic	87.24%	698.96	0.12	0.71
Green plastic	64.04%	699.97	0.06	0.14
Red plastic	68.30%	699.97	0.13	0.07

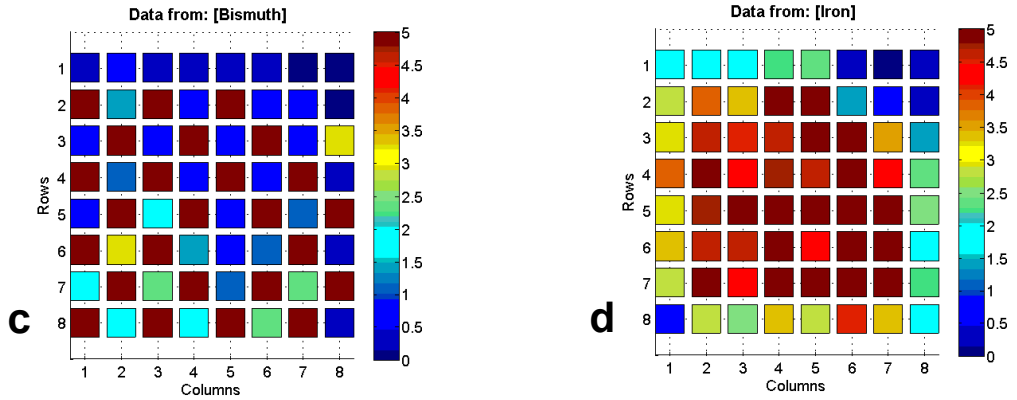

Figure 7. (a) Photocurrents of $BiVO_4$ (blue) and Fe (SL) (red) with all of the filters. Horizontal lines show the average photocurrent from scans without a filter. (b) Table of the average photocurrent detected from scans without a filter and with each filter. The maximum transmittance within the visible light spectrum also shown. (c) Bitmap of the SMD scan of $BiVO_4$ without a filter. (d) Bitmap of the SMD scan of Fe (SL) without a filter.

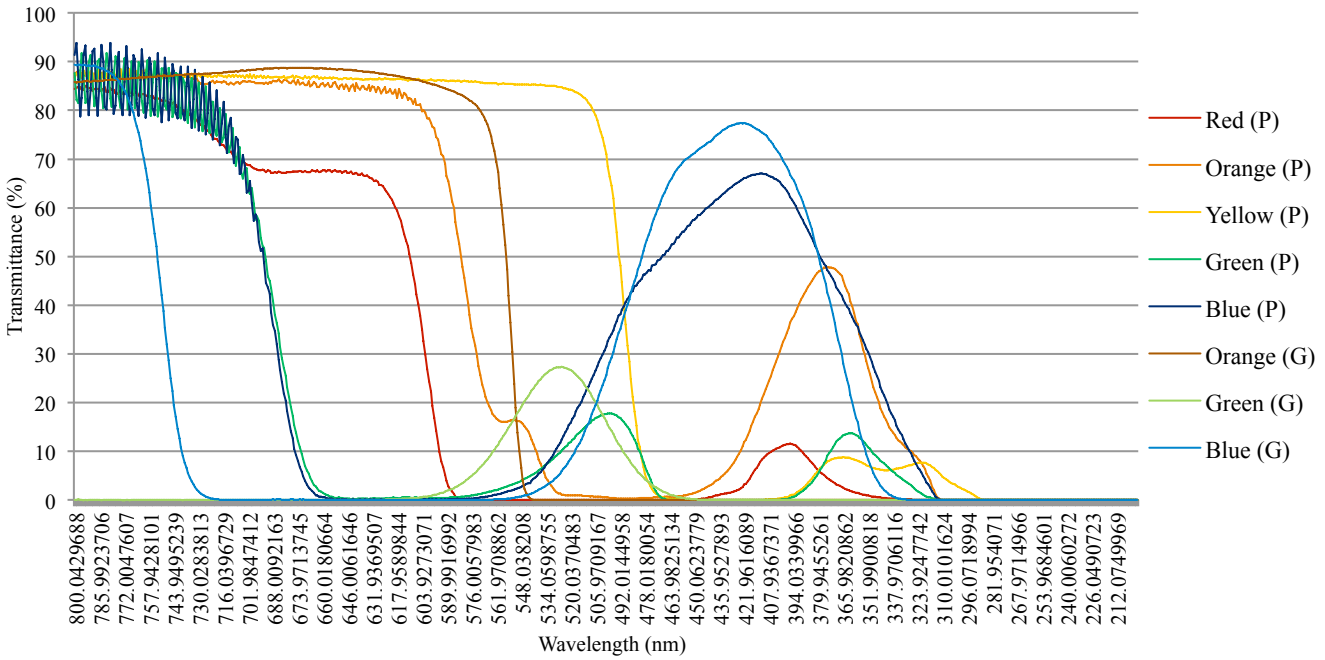

Figure 8. Transmittances of all filters, plastic gelatin (P) and glass (G), at the correlating wavelengths from 800 nm to 200 nm.

green filters led to much lower photocurrents; the green plastic filter scans often performed more poorly than the yellow plastic filter scans while the green glass filter scans often produced photocurrents very similar to those in the orange glass filter scans.

4. DISCUSSION.

4.1. Effects of the Optical Filters. The blue filter scans had the best performance because the blue filter transmitted the shortest and most energetic wavelengths to the plate. The scans without a filter did the best because unlike the scans with the filters, the no filter allowed all LED wavelengths illuminate the plate instead of restricting them, continuing with the belief that more light correlates with higher photocurrent. The order of performance for the plates showed that the majority of the detected photocurrent was due to the spots' photoactivity. But, a small portion of the photocurrent might have been due to photocorrosion because of the small photocurrent detected from scans with filters transmitting lower wavelengths than that of the band gap.

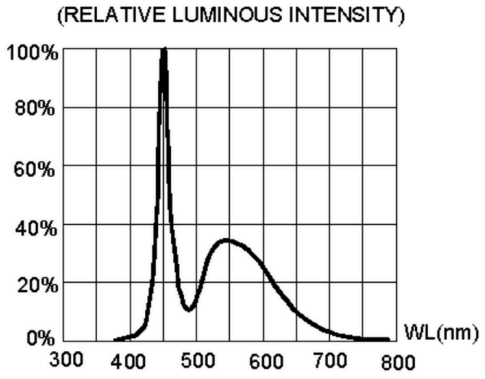

Figure 9. The relative luminous intensity of the wavelengths emitted by the LED lights[11].

4.2. Effects of Transmittances (UV-Vis). It was then discovered that green of both glass and plastic had very low transmittance, accounting for the low photoactivity that was unlike what was predicted. The scans with the green filters did not have as high photocurrent as expected due to the low transmittance. The green plastic filter had a maximum transmittance of 17.75% at 499.00 nm within the green light range (64.04% at 699.97 within the entire visible light range) and the green glass filter had a maximum transmittance of 27.31% at 525.02 nm. It can also be seen that the percent transmitted is slightly more important than the wavelength; scans with the green glass filter consistently led to higher photocurrent than scans with the green plastic filter despite the green plastic filter transmitting shorter wavelengths (Figure 8).

The intensity of the wavelengths emitted by the pulsing LED lights may have also caused unpredicted lower photocurrent from the green filter scans (Figure 9). The sudden lower transmittance at approximately 500 nm correlates with the wavelength range transmitted by both the green glass and green plastic filter. Also, the increase of intensity at approximately 550 nm possibly explains why the orange plastic filtered scans led to higher photocurrent than the orange glass filtered scans. The orange plastic filter has an increase in transmittance at 550 nm, despite having lower transmittance overall.

4.3. Why the Other Metal Oxides Resulted in Lower Photocurrents. It is suspected that the other metal oxides had an inferior performance compared to iron because the SEAL kit tests for both light absorption and catalytic properties, and these metal oxides were potentially good catalysts, but inadequate light absorption. The CuFe plate has a higher photocurrent compared to the other metal oxides most likely because of the large quantity of iron oxide mixed in. It is also believed that the 6:4 ratio performed better than the 8:2 and the 2:8 ratio performed better than the 4:6, despite their lower quantities of iron oxide, because the iron oxide formed a coffee ring around the main spot for the 8:2 and 4:6, leading to more copper oxide catalyzing.

4.4 Effects of Different Cleaning Methods. The standard cleaning method of rinsing the FTO plate with isopropanol and deionized water only eliminates only the dust from the plate. However, the ozone cleaning removed everything, which increased how hydrophilic the plate was. This induced the spreading of solution, which promoted the formation of a thin layer of solution. The thin layer allowed the solution to anneal better to the plate and formed non-crystallized spots, allowing the metal oxide to catalyze better.

4.5. Different Photoactivities with Iron Oxide.

4.5.1. Effects of Concentration. CON 2 performed with higher unfiltered photocurrent of almost 3 times more than CON 1 due to the higher molarity of the iron nitrate used. The higher molarity ensured that there would be more iron oxide on the plate to be tested. Since 0.4 M led to a higher photocurrent, 0.4 M was used for the majority of the succeeding plates. However, it was discovered that the higher molarity led to slower evaporation rates for the plate due to the abundance of iron nitrate molecules preventing the water molecules from being energetic enough to form a gas. As such, it was determined that 0.2 M be used for subsequent plates to optimize both the evaporation rate and photocurrent detected.

4.5.2. Effects of Surface Area. The increased surface area from the spread plates (NiFe 1, Fe (S), and Fe (SL)) allowed more iron oxide to be illuminated with each LED flash. Though the catalyst itself isn't necessarily better, the increased surface area ensures that there is more iron oxide catalyzing. This allows the results of the different filters to have a significant enough difference.

4.5.3. Effects of Crystallization. CON 3 performed similarly with CON 1 despite the higher molarity due to the crystallization of the iron oxide spots, forming the crystallized hematite. This crystallized form consisted of shiny, flaky spots that were not adhered to the plate and corroded into the electrolyte solution. The photocorrosion swept away most of the sample, not allowing most of the sample to be tested. After the photocorrosion, the spot was left with a small ring of non-crystallized iron oxide, which caused the majority of the photocurrent.

4.6. Bismuth Vanadate Compared to Iron Oxide. The band gap of bismuth vanadate is 2.4 eV while the band gap of iron (II, III) oxide is 2.18 eV. As seen in Chart GAH, both $BiVO_4$ and Fe (SL) began producing significantly higher photocurrent with the blue glass filter. $BiVO_4$ regularly had lower photocurrent with the other filters compared to Fe (SL), yet had higher photocurrent with the blue glass. This shows that iron oxide could possibly be a better light absorber than bismuth vanadate while bismuth vanadate could be a better catalyst. If this is true, then good catalysts could potentially be predicted based on how sharply the photocurrent rises once the wavelength correlating to the band gap is transmitted whereas good light absorbers could be identified on the slower ascendance of photocurrent.

4.7. Photoactivity Versus Photocorrosion. Based on how the blue filtered scans produced the highest photocurrent relative to the other filtered scans, it seems that the majority of the photocurrent detected is from photoactivity of the samples. There is also most likely a small percentage of photocorrosion that contributes to the spots, seen by the existent photocurrent from the scans with longer wavelength filters. However, it cannot be determined for certain if this is true because photocorrosion could increase as the wavelengths illuminating the plate shorten. Also, the disparities between the transmittances of the filters and the uneven wavelength intensity emitted by the LED lights show how the data gathered may be slightly inaccurate.

5. CONCLUSION

To investigate the possibility of photocorrosion causing the photocurrent detected by the SEAL kit, optical band-pass filters were used to restrict the wavelengths transmitted to the sample. It was discovered that iron oxide and bismuth vanadate produce high enough photocurrent to distinguish the difference in results of each of the filters. The photocurrents from the filtered scans tended to be lower with the longer wavelength filters and higher with the shorter wavelength filters. However, due to varying transmittances of the filters and the irregular distribution of wavelengths emitted by the LED lights, some filters led to unexpected results that did not follow the predicted trend. Since the majority of results proceeded as predicted, it seems that photoactivity of the samples contributes to the majority of the photocurrent. But, it cannot be confirmed because of other potential variables. In the future, other filters will be used to more accurately pinpoint the band gap of the samples. A black or grey filter may also be used later on to accommodate the different transmittances.

ASSOCIATED CONTENT

Supporting Information. Details of testing metal oxides, optical band-pass filters, SEAL kit, photocorrosion. This material is available free of charge via the Internet at http://pubs.acs.org.

AUTHOR INFORMATION

Corresponding Author

*angelinaye1217@gmail.com

Author Contributions

C. S. Delgadillo contributed equally to the creation of this work.

Notes

The authors declare no competing financial interest.

ACKNOWLEDGMENT

We thank Prof. Harry Grey and California Institute of Technology for funding and providing a laboratory for this research. We also thank Michelle DeBoever and Jacqueline Maslyn for supporting this research. This work was supported by the National Science Foundation (NSF) through the CCI Solar Fuels Outreach Program (CHE-1305124).

ABBREVIATIONS

SEAL, Solar Energy Activity Laboratory; FTO, fluorine-doped tin oxide

REFERENCES

(1) Egelstaff, J. How does solar power compare to other energy sources? *Solar Powered in Toronto*, **2015**

(2) Lewis, N. S.; Nocera, D. G. Powering the planet: Chemical challenges in solar energy utilization *Proc. Natl. Acad. Sci. U. S. A.*, **2006**, *103*, 15729-15735

(3) Van Coppenolle, L. Solar Energy Facts You Should Know *Texas Solar Energy Society*

(4) Winkler, G. R.; Winkler, J. R. A light emitting diode based photoelectrochemical screener for distributed combinatorial materials discovery *Rev. Sci. Instrum*., **2011**, *82*, 114101

(5) Bard, A. J.; Fox, M. A. Artificial Photosynthesis: Solar Splitting of Water to Hydrogen and Oxygen *Acc. Chem. Res.,* **1995**, *28*, 141-145

(6) McKone, J. R.; Ardo, S.; Blakemore J. D.; Bracher, P. J.; Dempsey, J. L.; Darnton, T. V.; Hansen, M. C.; Harman, W. H.; Rose, M. J.; Walter, M. G.; Dasgupta, S.; Winkler, J. R.; Gray, H. R. The Solar Army: A Case Study in Outreach Based on Solar Photoelectrochemistry *Rev. Adv. Sci. Eng.,* **2014**, *3*, 288-303

(7) McKone, J. R.; Lewis, N. S.; Gray, H. R. Will Solar-Driven Water-Splitting Devices See the Light of Day? *Am. Chem. Soc*., **2014**, *26*, 407-414

(8) DeBoever M. C. SEAL Experiment *The Solar Army*, **2015**

(9) Barlow, J.; Thin films of nickel and iron oxides yield efficient solar water-splitting catalyst *University of Oregon*, **2013**

(10) Park, Y.; McDonald, K. J.; Choi, K. S. Progress in bismuth vanadate photoanodes for use in solar water oxidation *Chem. Soc. Rev*., **2013**, *42*, 2321-2337

(11) OPTEK Technology, Inc. White High-Intensity LED Lamp. *TT Electronics*, 4